

8<sup>th</sup> International Conference on Photonic Technologies LANE 2014

## Laser cladding of TiAl intermetallic alloy on Ti6Al4V. Process optimization and properties.

B. Cárcel<sup>a,\*</sup>, A. Serrano<sup>a</sup>, J. Zambrano<sup>b</sup>, V. Amigó<sup>c</sup>, A.C. Cárcel<sup>c</sup>

<sup>a</sup>AIDO, Spain

<sup>b</sup>Centro de Investigaciones en Materiales (CIM), Universidad de Carabobo, Venezuela

<sup>c</sup>Instituto de Tecnología de Materiales (ITM - UPV), Spain

---

### Abstract

In order to improve Ti6Al4V high-temperature resistance and its tribological properties, the deposition of TiAl intermetallic (Ti-48Al-2Cr-2Nb) coating on a Ti6Al4V substrate by coaxial laser cladding has been investigated. Laser cladding by powder injection is an emerging laser material processing technique that allows the deposition of thick protective coatings on substrates, using a high power laser beam as heat source. Laser cladding is a multiple-parameter-dependent process. The main process parameters involved (laser power, powder feeding rate, scanning speed and preheating temperature) has been optimized. The microstructure and geometrical quantities (clad area and dilution) of the coating was characterized by optical microscopy and scanning electron microscopy (SEM). In addition the cooling rate of the clad during the process was measured by a dual-color pyrometer. This result has been related to defectology and mechanical coating properties.

© 2014 Published by Elsevier B.V. This is an open access article under the CC BY-NC-ND license (<http://creativecommons.org/licenses/by-nc-nd/3.0/>).

Peer-review under responsibility of the Bayerisches Laserzentrum GmbH

*Keywords:* Laser; Cladding; TiAl; Titanium; TBC

---

### 1. Introduction

The improvement of energy efficiency and power in turbomachines (used in aeronautical industry as well as in power generation industry) is related to the increase of their maximum work temperature, requiring the development of materials with high temperature resistance. A way to achieve high temperature resistance is the development of

---

\* Corresponding author. Tel.: +34-961318051; fax: +34-961318007.  
E-mail address: [bcarcel@aido.es](mailto:bcarcel@aido.es)

coatings with good high temperature performance suitable to work as Thermal Barrier Coatings (TBCs). TBCs provide thermal insulation to base materials and protect them against corrosion and erosion at high temperatures Osorio *et al* (2012). Laser cladding has received significant attention in recent years. It offers many advantages over conventional coating processes (e.g. arc welding or plasma spraying): Laser cladding technology allows the deposition of quality metal coatings providing high accuracy and low thermal effect of the base material. The process involves the melting of powder with high power lasers on a substrate, so that the dilution of the fed material provides excellent metallurgical coating adhesion. Toyserkani and Khajepour (2005).

Nowadays, the Ti-6Al-4V alloy is by far the most popular titanium alloy. Over 50% of all Ti alloys in use are made of Ti-6Al-4V, but its use is limited to temperatures below 400°C. In order to increase temperature operation of this material, intermetallic TiAl coatings are studied in this investigation. Titanium-Aluminum intermetallic alloys are materials for high temperature applications (operating temperature between 600-760°C) due to its high melting point (1440°C), low density, high elastic modulus and good structural stability, besides its specific resistance is higher than titanium alloys and equal to that of the nickel-based superalloy. Leyens and Peters (2003), Huang *et al* (2012).

The aim of this work is to optimize and analyze laser cladding coatings of TiAl intermetallic alloy on Ti6Al4V.

## 2. Experimental procedure

The powders used in this study were Ti-48Al-2Cr-2Nb (%at.), supplied by TLS Technik with particle size between 100-200 µm. Rectangular Ti-6Al-4V sheets were used as base material.

In order to study the effects of the main laser cladding parameters (laser power, powder feeding rate, scanning speed and preheating temperature), single clad track experiments were initially performed. Laser power were tested in the range of 500-900 W, with scanning speed between 100-600 mm/min and powder feeding rate between 1-4 g/min.. Based on optimized single track results, multiple track coating were carried out.

The experimental setup is illustrated in Fig. 1. Laser cladding system consisted of Nd:YAG laser (wavelength 1064 nm) TRUMPH model HL1006D with a maximum output power of 1kW. The light is guided through an optical fibre of 0.6 mm of core diameter to the laser head containing the optical system with a focusing lense of 200 mm. The optical system is assembled to the cladding coaxial nozzle. For this investigation the laser diameter was set to 2 mm, the samples were place 8 mm from the cladding nozzle. For feeding the additive material a dispensing system Sulzer Twin 10C was used. The motion system consist of 4 stages XYZC commanded by a Siemens digital CNC.

The substrate has been preheated by a heating plate before and during the cladding process at 350 or 450 °C (in order to prevent undesirable alterations on the substrate microstructure, preheating temperatures were set below 500°C). The time-dependent temperature of the tracks were measured using a digital highly accurate IMPAC Igar 12-LO two-color pyrometer capable of measuring temperatures in the range of 550-2500 °C.

Temperature was measured in a fixed point of the track. Temperature data was converted into graphs with Microsoft Excel software. From these graphs cooling rate of each track were calculated.

After laser cladding process the coatings were evaluated by penetrating fluid (NDT) for the observation of possible macroscopic defects. PFINDER 860 colour contrast penetrant and PFINDER 870 developer were used.

In order to analyze the microstructure and geometrical quantities of the coatings, metallographic samples were prepared. The specimens were cut transverse to the clad direction. They were prepared using standard mechanical polishing procedures and etched in a solution of 92% H<sub>2</sub>O, 2.5% HF and 5.5% HNO<sub>3</sub>. Metallographic samples were inspected by a confocal microscopy LeicaSCAN DCM3D and ImageJ image analysis software was used.

SEM analysis was carried out with a JEOL JSM 6300 scanning microscope, including microanalysis by EDX.

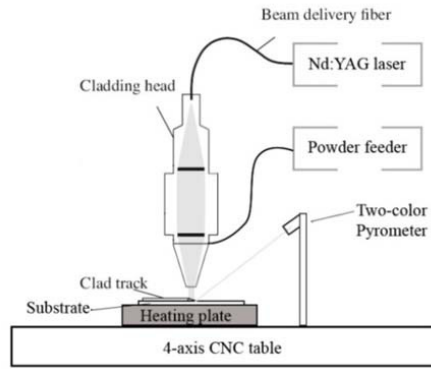


Fig. 1. Schematic overview of the laser cladding system.

For single laser track geometrical characterization, the main variables of the cross section of laser track have been measured (Fig. 2). These are: clad height  $H$  ( $\mu\text{m}$ ), clad width  $W$  ( $\mu\text{m}$ ), clad area  $A_c$  ( $\mu\text{m}^2$ ) and molten area  $A_m$  ( $\mu\text{m}^2$ ). From these, dilution  $D=A_m/(A_c+A_m)$  and aspect ratio  $AR=W/H$  has been calculated. Mechanical coating properties are measured by microhardness testing, carried out with a Vickers microhardness machine (HV0.1/10) according to ISO 4516.

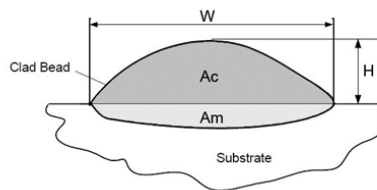


Fig. 2. Cross section of laser track: main geometrical quantities. (Clad height  $H$ , clad width  $W$ , clad area  $A_c$  and molten area  $A_m$ ).

### 3. Results and discussion. Laser cladding of single tracks.

#### 3.1. Geometrical analysis

The most important geometric characteristics of a laser track are dilution and aspect ratio. Aspect ratio is related with the appearance of porosity and cracking in overlapping tracks. In order to ensure a good overlapping, aspect ratio between 3 and 5 is advisable. Steen (2003). On the other hand, dilution quantifies the relative amount the substrate material that has been molten during the cladding process and mixed with the clad material. The aim of laser cladding is to cover one metal with another to form an interfacial bond without diluting the cladding metal with substrate material giving that dilution may degrade coating properties, although some dilution is required to guarantee a good metallurgical bond. De Oliveira *et al* (2005).

As shown in Table 1, tracks carried with a powder feeding rate of 2g/min have higher aspect ratios (greater than 5) that tracks performed at 4g/min (under 5). In addition, values of dilution in tracks 1 to 9 are very high (between 15 - 40%) and for tracks 10 to 18 the dilution is almost negligible, i.e. dilution increases with decrease in the powder feeding rate.

Based on cooling rate measurements and NDT testing (Penetrant Fluid) a second set of tests were carried out decreasing scanning speed in order to reduce cooling rate and therefore cracking in the coatings.

Table 1. Processing parameters and geometrical quantities of tracks. SET 1.

Track	Laser Power (W)	Scanning Speed (mm/min)	Power Feeding Rate (g/min)	350°C				450°C			
				Width ( $\mu\text{m}$ )	Height ( $\mu\text{m}$ )	Aspect Ratio (w/h)	Dilution (%)	Width ( $\mu\text{m}$ )	Height ( $\mu\text{m}$ )	Aspect Ratio (w/h)	Dilution (%)
1	700	300	2	2744	508	5,4	15,0%	2779	536	5,2	15,2%
2	800	300	2	3035	550	5,5	16,8%	3123	532	5,9	20,3%
3	900	300	2	3297	595	5,5	22,6%	3397	550	6,2	24,9%
4	700	450	2	2518	375	6,7	21,1%	2547	386	6,6	23,1%
5	800	450	2	2770	430	6,4	26,5%	2822	371	7,6	34,3%
6	900	450	2	2994	427	7,0	31,3%	3102	389	8,0	35,3%
7	700	600	2	2327	332	7,0	28,2%	2391	272	8,8	33,3%
8	800	600	2	2567	324	7,9	37,2%	2623	324	8,1	33,2%
9	900	600	2	2789	363	7,7	38,0%	2839	322	8,8	43,1%
10	700	300	4	2734	1131	2,4	0,0%	2999	1017	3,0	0,0%
11	800	300	4	3008	1195	2,5	0,0%	3110	1024	3,0	1,5%
12	900	300	4	3341	1175	2,8	1,6%	3393	1068	3,2	6,7%
13	700	450	4	2442	827	3,0	2,0%	2586	734	3,5	0,0%
14	800	450	4	2714	826	3,3	2,2%	2792	735	3,8	6,4%
15	900	450	4	2977	872	3,4	2,8%	2993	786	3,8	10,4%
16	700	600	4	2270	634	3,6	0,0%	2434	596	4,1	6,6%
17	800	600	4	2465	689	3,6	4,7%	2596	594	4,4	10,0%
18	900	600	4	2680	722	3,7	5,8%	2800	616	4,5	16,5%

Table 2. Processing parameters and geometrical quantities of tracks. SET 2.

Track	Laser Power (W)	Scanning Speed (mm/min)	Power Feeding Rate (g/min)	350°C			
				Width ( $\mu\text{m}$ )	Height ( $\mu\text{m}$ )	Aspect Ratio (w/h)	Dilution (%)
1	600	100	1	3323	801	4,1	11%
2	500	100	1	2744	843	3,3	6%
3	400	100	1	2216	963	2,3	2%

### 3.2. Non-destructive testing. Penetrant testing (PT)

In the following figure results of penetrating fluid test are shown. This non destructive test was carried out in order to analyze cracking in single tracks and coatings.

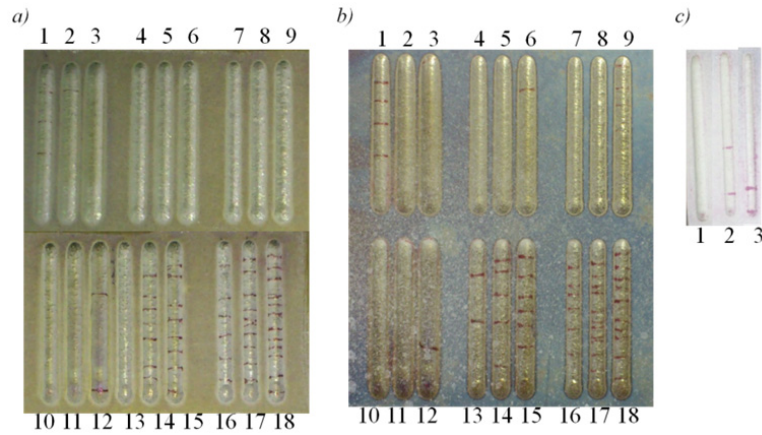


Fig. 3. Penetrating fluid test results for single tracks. (a) SET 1- Preheating temperature= 350°C; (b) SET 1- Preheating temperature= 450°C; (c) SET 2. (Process parameters in Table 1 and Table 2).

Single tracks samples after PT are shown in figure 3. Cracking is clearly higher for higher powder feed rate and for higher processing velocity. No important differences have been observed based on preheating temperature.

From this preliminary optimization tests, tracks number 1 and 2 (SET 1) corresponding to a powder feeding rate of 2g/min and scanning speed of 300 mm/min, dilution about 15% and aspect ratio is 5, were the best in terms of defectology for the combined with acceptable geometrical characteristics. Other tracks free of cracks (i.e 10, 11) showed lack of adhesion. For the second set (SET 2) of tests, track number 1 was clearly the best, being the only one without cracks.

### 3.3. Pyrometry

The following figure shows a single track temperature evolution. Three zones are shown: heating zone, liquid phase cooling and solid phase cooling zone. The liquid to solid transition is given about the temperature of 1450 °C.

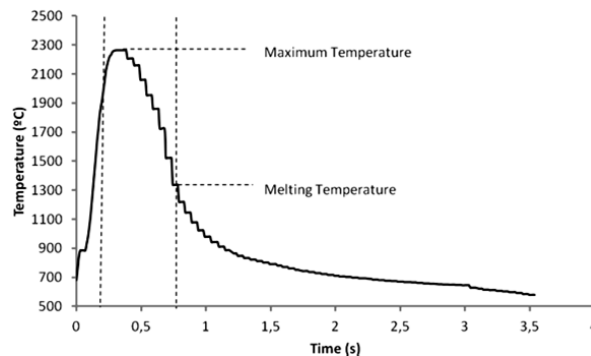


Fig. 4. Temperature evolution for a track.

The cooling rate has been measured in the solid phase as the average cooling speed between 1450 and 800°C. Results have been adjusted to a potential curve, so temperatures (°C) versus time (s) graphs are plotted.

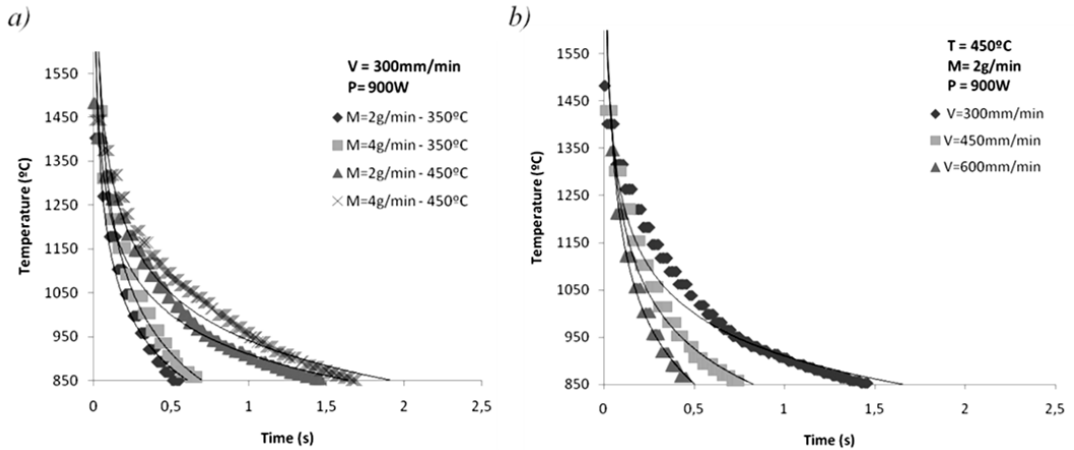


Fig. 5. Temperature vs time graphs. (a) Depending on Power feeding rate and Preheating temperature; (b) Depending on Scanning speed. Cooling rates: (a) 466, 371, 323, 292 °C/s; (b) 1120, 723, 323 °C/s.

Cooling rate is affected by scanning speed. As shown in Fig.3, the cooling rate of the material increases considerably for higher scanning speed. The increase of cooling rate has a significant effect on the quality of tracks. This way, cracking defectology decreases for tests with lower scanning speed (300 – 100 mm/min). As far as heating temperature is concerned, significant differences are not observed between 350°C and 450°C.

### 3.4. Mechanical properties. Microhardness.

For this study the microhardness of single tracks has been measured. Results showed that, as shown in figure 6, hardness usually increases with scanning speed, related with higher cooling rates. It has been found through studies of spark plasma sintering processes in TiAl, that when very rapid cooling are presented microstructures are generated out of balance, with hardness values similar to those obtained. Xiao et al (2009), Xiao et al (2012).

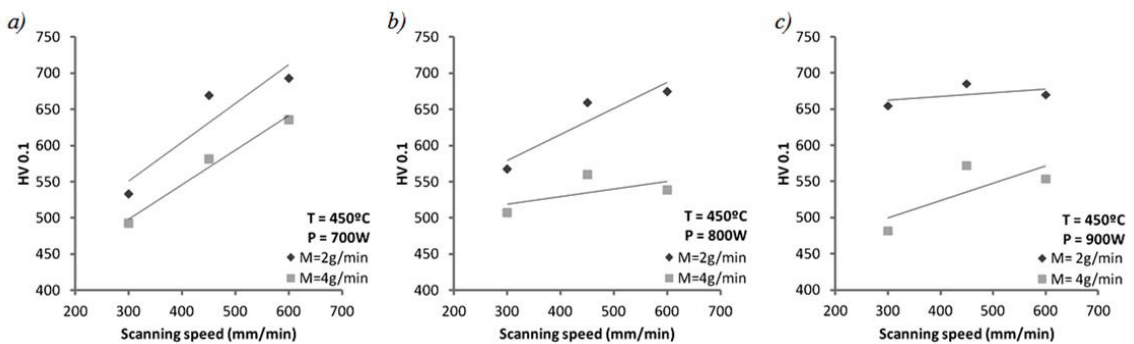


Fig. 6. Microhardness testing as function of Scanning speed. (a) Power= 700W; (b) Power= 800W; (c) Power= 900W.

#### 4. Results and discussion. Laser cladding coating.

##### 4.1. Geometrical analysis and microstructure.

Optimized coating based on single track 1 (set 2), with an overlapping of 40% was carried out (50 x 50 mm), obtaining a coating thickness of 950  $\mu\text{m}$ . Although no measurements of distortion were carried out on processed samples, visual inspection reported little deformation of samples, below the range of the coating thickness.

Metallographic inspection (Fig. 7) showed a non-uniform dendritic microstructure. Small isolated porosity (< 50  $\mu\text{m}$ ) between tracks have been observed.

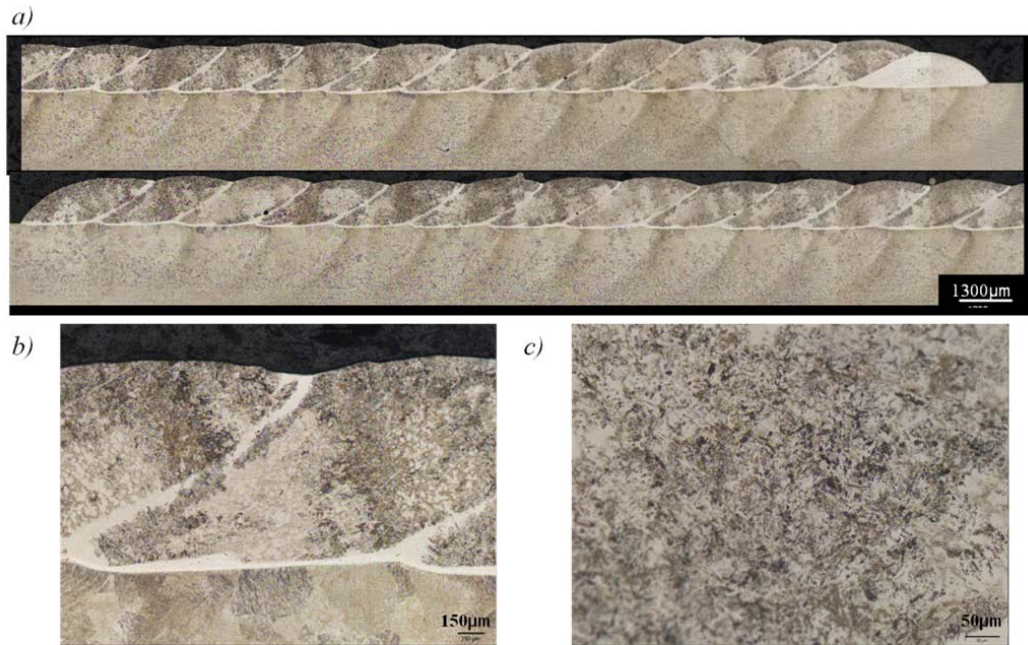


Fig. 7. Optical microscopy images. (a) Overall image of coating; (b) Interface; (c) Coating.

Scanning Electron Microscopy (SEM) images are shown in figure 8. The coating showed a fine dendritic microstructure (second arm spacing <0.5  $\mu\text{m}$  - Fig. 8b). In order to measure the composition of the coating and base material (HAZ), three regions were measured by EDS: coating material, interface and base material (Fig. 8c – table 3).

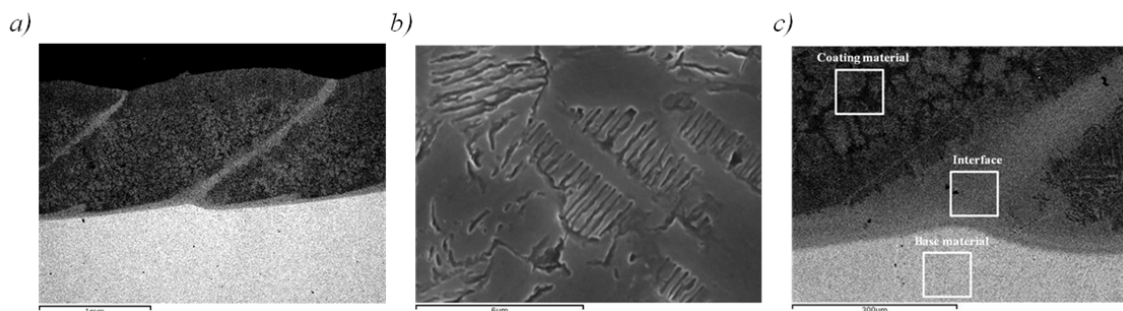


Fig. 8. SEM micrographs. (a) Overall image of coating; (b) Dendritic microstructure; (c) Microanalysis regions.

Table 3. Microanalysis results.

Regions	Weight%					Atomic%				
	Al	Ti	V	Cr	Nb	Al	Ti	V	Cr	Nb
Coating material	31.60	60.95		2.59	4.87	46.00	49.98		1.96	2.06
Interface	29.06	63.34		2.18	5.42	43.08	52.91		1.68	2.33
Base material	6.06	90.07	3.87			10.30	86.22	3.48		

There is an interface between tracks (thickness in the range of  $100\mu\text{m}$ ) in the same way that the interface between coating a base material. This interface is richer in Ti (Ti-43Al-1.7Cr-2.3N at.%) than the overall coating, being a transition zone with the base material. Coating composition (Ti-46Al-2Cr-2Nb at.%) is close to the composition of the original powder (Ti-48Al-2Cr-2Nb at.%) but slightly richer in Ti due to dilution with base material. Base material showed the expected composition according with reference (Ti-6.06Al-3.87V wt.%). (Table 3).

#### 4.2. Non-destructive testing. Penetrant Testing (PT)

The best coatings in terms of lack of cracking have been obtained for low scanning speed ( $100\text{ mm/min}$ ). Single tracks and small coatings based on processing parameters shown in table 2 (Set 2) have been obtained without cracking (NDT). (Fig. 9).

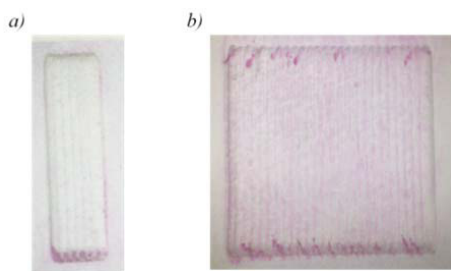


Fig. 9. NDT optimized coatings (a) Small coating based on track 1 (SET 2); (b) TiAl optimized coating (50x50mm).

#### 4.3. Mechanical properties. Microhardness.

Transverse measurements were performed from  $0.2\text{ mm}$  under the laser cladding coating surface to the base material with a vertical distance between measurements of  $0.2\text{mm}$  (Fig. 9a). The average hardness of the coating is  $430\text{HV}$  higher than hardness of the substrate. Moreover, when compared with the hardness of the tracks having a lower hardness, this is because the coatings have a lower cooling rate and it is related to the microstructure obtained. Guyon *et al* (2013)



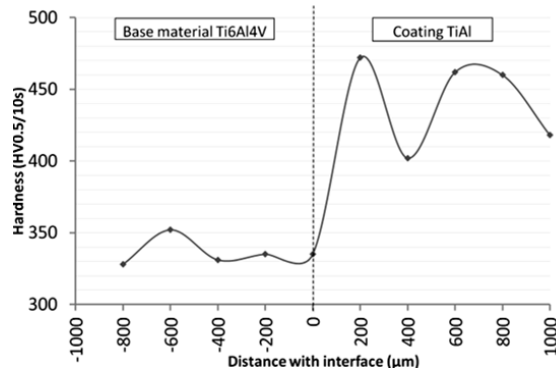


Fig. 10. Microhardness testing.

## 5. Conclusions

Laser cladding of TiAl intermetallics on Ti6Al4V alloy has shown to be a suitable technique for the development of TBCs only under specific processing conditions, limited by the brittle behavior of the intermetallic.

Several tests have been carried out in order to obtain defect free coatings with good adhesion and mechanical properties. The main conclusions are listed:

- Cracking has shown to be the main defectology issue to overcome in the laser cladding processing of TiAl
- Heating previously and during the process improves the results in terms of cracking.
- Cooling rate (measured by 2c-pirometry) affects the mechanical properties (hardness) and defectology (cracking) of the tracks and coatings. Higher cooling rates are related with higher hardness but in the same way is the cause to an increase in cracking.
- A direct relation has been found between cooling rate and input parameters like scanning speed. This way the process has been optimized minimizing the cooling rate by decreasing the scanning speed of the process.
- TiAl coating obtained by laser cladding showed a fine dendritic microstructure. Good metallurgical bonding is observed by OM and SEM. There is a clear interface between the coating and base material and also between tracks. The composition of the coating is similar to the composition of the additive powder with a little increase in Ti due to dilution.
- The microhardness measured in the coating (aprox. 430 HV) is higher than the typical hardness of TiAl cast alloys (aprox. 250-300 HV). This effect is related with a higher cooling rate.

## Acknowledgements

The authors gratefully acknowledge the financial support of Spanish Ministry of Economy and Competitiveness MINECO, National R+D program, to this project (MAT2011-28492-C03).

## References

- Osorio J.D., Toro A., Hernández-ortiz J.P., 2012. Thermal barrier coatings for gas turbine applications: failure mechanisms and key microstructural features. *Dyna* 176, 149-158.
- Toyserkani, E., Khajepour, A., 2005. *Laser cladding*. (Ed) CRC Press.
- Leyens C. and Peters M. (Eds.). *Titanium and Titanium Alloys, fundamentals and applications*, WILEY-VCH, ISBN: 3-527-30534-3, (2003), pp. 343
- Huang Y, Wang Y, Fan H, Shen J, A. 2012. TiAl based alloy with excellent mechanical performance prepared by gas atomization and spark plasma sintering, *Intermetallics* 31, 202-207.
- Steen W.M., 2003. *Laser Materials Processing*, Springer Verlag, London, 320-329
- De Oliveira U, Ocelik V, De Hosson J. Th. M. 2005. Analysis of coaxial laser cladding processing conditions, *Surface & Coatings Technology*, 197, 127-136.
- Xiao S, Tian J, Xu L, Chen Y, Yu H, Han J. 2009. Microstructures and mechanical properties of TiAl alloy prepared by spark plasma sintering, *Trans. Nonferrous Met. Soc. China* 19, 1423-1427
- Xiao S, Xu L, Chen Y, Yu H. 2012. Microstructure and mechanical properties of TiAl-based alloy prepared by double mechanical milling and spark plasma sintering. *Trans. Nonferrous Met. Soc. China* 22, 1086-1091
- Guyon J, Hazotte A, Monchoux J, Bouzy E. 2013. Effect of powder state on spark plasma sintering of TiAl alloys. *Intermetallics* 34, 94-100